REPORTS OF PRACTICAL ONCOLOGY AND RADIOTHERAPY 18 (2013) 173–178

Available online at www.sciencedirect.com

SciVerse ScienceDirect

journal homepage: http://www.elsevier.com/locate/rpor

Original research article

Initial evaluation of intrafraction motion using frameless CyberKnife VSI system

Alejandro Floriano, Icíar Santa-Olalla, Alberto Sanchez-Reyes*

Department of Medical Physics, CyberKnife Unit, IMO Group Radiotherapy and Robotic Radiosurgery Center, Madrid, Spain

ARTICLE INFO

Article history:
Received 13 September 2012
Received in revised form
21 December 2012
Accepted 17 March 2013

Keywords:
Robotic radiosurgery
Frameless
Intrafraction movement
Accuracy

ABSTRACT

Aim: To analyze intrafraction movement in patients undergoing frameless robotic radiosurgery and evaluate the influence of image acquisition frequency on global accuracy.
Background: Stereotactic radiosurgery requires high spatial accuracy in dose delivery. In conventional radiosurgery, a rigid frame is used to guarantee a correct target alignment and no subsequent movement. Frameless radiosurgery with thermoplastic mask for immobilization cannot completely eliminate intrafraction patient movement. In such cases, it is necessary to evaluate its influence on global treatment accuracy.
Materials and methods: We analyzed the intrafraction motion of the first 15 patients undergoing intracranial radiosurgery (39 fractions) with the CyberKnife VSI system at our institution. Patient position was measured at a 15–90-s interval and was used to estimate intrafraction patient movement.
Results: With our acquisition image protocol and immobilization device, the 99% displacement error was lower than 0.85 mm. The systematic movement components were lower than 0.05 mm and the random component was lower than 0.3 mm in the 3 translational axes. Clear linear time dependence was found in the random component.
Conclusions: Selection of the X-ray image acquisition time is necessary to meet the accuracy required for radiosurgery procedures with the CyberKnife VSI system. We verified that our image acquisition protocol met the 1-mm criterion.

1. Background

Radiosurgery delivers high-dose radiation with adequate coverage of the target, high dose conformation, and high gradient.[1,2] An accuracy of between 1 mm and 2 mm in dose placement[1,2] is widely accepted. Linear accelerator-based cranial stereotactic radiosurgery uses a rigid frame device to immobilize the head and to define the coordinate system necessary to localize the target.

* *Corresponding author at*: Department of Medical Physics, CyberKnife Unit, IMO Group Radiotherapy and Robotic Radiosurgery Center, C/Emilio Vargas, 16, 28053 Madrid, Spain. Tel.: +34 915155354; fax: +34 914161691.
E-mail addresses: afloriano@grupoimo.com (A. Floriano), asantaolalla@grupoimo.com (I. Santa-Olalla), asanchezreyes@grupoimo.com (A. Sanchez-Reyes).
1507-1367/$ – see front matter © 2013 Greater Poland Cancer Centre. Published by Elsevier Urban & Partner Sp. z o.o. All rights reserved.
http://dx.doi.org/10.1016/j.rpor.2013.03.004

However, image-guided frameless radiosurgery techniques are also capable of delivering high doses with submillimeter accuracy.[3–6] The CyberKnife VSI™ System (Accuray Incorporated, Sunnyvale, CA, USA) eliminates the use of invasive frame fixation by detecting and adjusting for patient movement during treatment delivery. Unlike frame radiosurgery, where the absence of movement and subsequent submillimeter setup accuracy are assumed, the use of a thermoplastic mask cannot completely eliminate intrafraction movement. This drawback necessitates 2 approaches: (a) an image registration method for the initial setup, with subsequent tracking and correction for intrafraction movements; and (b) a user X-ray acquisition procedure to guarantee the global 1–2-mm error.

The 2D–3D registration method implemented in the CyberKnife VSI system has an accurate initial set-up with constant adjustment for patient movement during image-guided intracranial radiosurgery. Phantom-based measurements have shown the registration error to be lower than 0.5 mm.[3]

Image acquisition, target localization, and alignment corrections are repeated continuously during the delivery. X-ray images acquired in real time and digitally reconstructed radiographs (DRR) are compared to detect any change in patient position with respect to the reference.[3,7,8] The robotic manipulator compensates for translations and rotations on the basis of the corrections obtained from the most recently acquired image pair, and the user can adjust the imaging interval during treatment. As the selection of the imaging interval is based on the stability of the target position during the fraction, our initial procedure involved selecting a minimum acquisition time from among images of between 15 and 60 s.

Patient movement patterns in CyberKnife VSI and their effect on dose alignment accuracy were studied using different types of analysis.[9,10] The results show a relationship between time and the systematic and random components of the intrafraction movements, leading the authors to conclude that acquisition interval is a key factor in an accurate dose delivery.

2. Aim

We present our findings on intrafraction patient movement for the first 15 patients undergoing intracranial radiosurgery using CyberKnife VSI at our center in order to analyze the initial image acquisition procedure. We compare our results with the well-established 1–2-mm accuracy of delivery as part of our quality assurance program.

3. Materials and methods

3.1. *Treatment delivery system*

Two diagnostic X-ray sources are mounted on the ceiling and 2 X-ray detectors sit flat on the floor. The amorphous silicon flat-panel X-ray detectors generate a high-resolution digital image (1024 × 1024 pixels, 16-bit resolution, and pixel spacing of 0.4 mm), which is registered using high-contrast bony anatomy in the field of view, with software corrections applied to eliminate the distortion due to the 45° angle between the detector and the central axis of the X-ray beam.[11] The registration algorithm determines the 3D rigid transformation required to align the patient's position with the treatment planning computed tomography (CT) image in the delivery coordinate system, using 2 sets of DRR images generated offline from the CT as a reference.[7] The current translational and rotational corrections obtained are applied using the robotic manipulator. Table 1 shows the nomenclature employed by the CyberKnife VSI system for the corrections in the coordinate frame of the room.

Table 1 – Room space coordinate nomenclature.

Translation	Rotation
SUP (X): superior(−) – inferior(+) axes	*ROLL* (Roll): X axes rotation
RGT (Y): left(+) – right(−) axes	*UP* (Pitch): Y axes rotation
OPOS (Z): anterior(+) – posterior(−) axes	*CW* (Yaw): Z axes rotation

3.2. *Patient population*

The initial study included the first 15 patients to receive intracranial radiosurgery at the CyberKnife VSI therapy unit in the Radiotherapy and Robotic Radiosurgery Center (IMO Group) between April 2011 and June 2011. The number of fractions per treatment ranged from 1 to 5 depending on the pathology, localization, and total dose delivered to the target. We recorded and analyzed 39 cranial fractions. All the patients were immobilized in the supine position, with a 2.4-mm-thick thermoplastic mask (LorcaMarín, S.A.) and headrest. A CT scan was carried out (125 kVp, 500 mA, and 1.25-mm slice thickness), and the secondary images necessary to define the target were acquired. Treatment was planned and administered for 13 out of 15 patients using the new IRIS collimator device, which can reduce the number of monitor units required, increase treatment speed, and improve the conformity and homogeneity of treatment plans.[12]

3.3. *Image guidance protocol*

Patient position was assessed from 2 orthogonal planar X-ray images. Before treatment, the patient was aligned using an adjustable couch to reduce the corrections required to below maximum robotic manipulator limits. CyberKnife VSI can correct translations of up to ±10 mm in the 3 axes and rotations of up to ±1.0° in the ROLL and UP axes and ±3.0° in the CW axes. The system enables the user to specify the minimum interval between image acquisitions within a range of 5–150 s during treatment. In our center, when acquisition starts, a default 15-s image interval is selected. After verifying target stability for the first few minutes, the imaging interval is increased progressively up to a 60-s minimum, depending on patient stability.

3.4. *Data source and collection*

During treatment, the CyberKnife VSI generates a data log file with information on acquisition time and the corrections applied by the robotic manipulator in the treatment

coordinate system. Translations and rotations are studied independently in each axis. For each fraction i, and each acquisition at a time t_j (with j as an integer), a patient displacement vector $\mathbf{r}_{ij}$ is obtained, with $\mathbf{r}_{ij} = (SUP, RGT, OPOS, ROLL, UP, CW)_j$. Patient movement and the associated beam misalignment between 2 consecutive images is estimated by the following equation:

$$\varepsilon_{ij} = r_{i,j+1} - r_{ij} \tag{1}$$

A global 3D misalignment error d is defined as the root sum square of the 3 translation components. The data sets were checked before the statistical analysis when necessary to eliminate abrupt shifts of the treatment couch, which are not associated with real patient movement.

3.5. *Data analysis*

Distribution of patient movement error was analyzed as a function of mean acquisition time. The systematic and random component of the distribution was calculated using an approach described elsewhere.[14] The systematic error for the fraction i can be obtained by

$$S_i^T = \frac{1}{N_{f,i}} \sum_{j=1}^{N_{f,i}} \varepsilon_{ij}^T, \tag{2}$$

where $N_{f,i}$ is the total number of images acquired in the fraction i.

The random error for the fraction i can also be estimated from

$$\sigma_i^T = \left[\frac{1}{N_{f,i} - 1} \sum_{j=1}^{N_{f,i}} (\varepsilon_{ij} - S_i^T)^2 \right]^{1/2}. \tag{3}$$

These values enabled us to obtain the mean population setup error as

$$\mu^T = \frac{1}{N_s} \sum_{i=1}^{N_s} S_i^T \tag{4}$$

and the population random error as

$$\sigma^T = \left[\frac{1}{N_s} \sum_{i=1}^{N_s} \sigma_i^2 \right]^{1/2} \tag{5}$$

where N_s is the total number of fractions included in the study.

Finally, the population systematic error is defined as the standard deviation of the patient systematic error, as follows:

$$\Sigma^T = \left[\frac{1}{N_s - 1} \sum_{j=1}^{N_s} (S_i^T - \mu^T)^2 \right]^{1/2} \tag{6}$$

We also investigated the effect of variations in acquisition frequency on accuracy, movement distribution, and error components by repeating the previous analysis (Eqs. (2)–(6)) with different skip factors between images in Eq. (1). Instead of calculating the misalignment between consecutive images ($\varepsilon_{ij} = r_{i,j+1} - r_{ij}$), we calculated the misalignment between alternate images (e.g., between 1 and 3, 2 and 4, etc. [$\varepsilon_{ij} = r_{i,j+2} - r_{ij}$]; between 1 and 4, 2 and 5, etc. [$\varepsilon_{ij} = r_{i,j+3} - r_{ij}$]; and between 1 and 5, 2 and 6, etc. [$\varepsilon_{ij} = r_{i,j+4} - r_{ij}$]). We thus generated hypothetical ε_{ij} distributions as if we had increased the interval time between acquisitions in a fraction.

Table 2 – Mean, systematic and random errors for each translational and rotational coordinate.

	μ^T (mm)	Σ^T (mm)	σ^T (mm)
SUP	0.022	0.042	0.202
RGT	−0.021	0.034	0.188
OPOS	0.014	0.015	0.137
ROLL	0.010	0.016	0.119
UP	0.006	0.025	0.167
CW	0.007	0.021	0.201

4. Results

4.1. *Distribution of patient in translation and rotation*

Fig. 1 shows the box plot for the 39 intracranial radiosurgery fractions obtained from the acquisition protocol used in our department. The graph shows that the smallest displacements are generally found for the OPOS translations and the ROLL rotations, although no significant variations in the movement pattern were observed between the axes. The advantage of this representation is that it reveals unusual movement patterns for a particular patient or fraction.

Fig. 2 shows the cumulative histogram for the translational components, together with the 3D misalignment global error, d. For the 3 components, 95% are below 0.5 mm, whereas for the 3D global error, 95% are below 0.7 mm.

4.2. *Systematic and random error components*

Table 2 shows the systematic and random components from the movement error distribution with our acquisition protocol calculated from Eqs. (4)–(6), specified by coordinates. The overall mean error was lower than 0.05 for all the translations and rotations, and the random error was the main contributor to global error in all cases. No particular direction of movement was observed, and values were similar for all the coordinates.

4.3. *Time dependence of translational and rotational motion distribution*

Using the simulated error distribution obtained with different skip factors between images, we were able to calculate the histogram and systematic and random errors. Fig. 3 shows the spread of the 3D global error histogram in the hypothetical case that we had increased the mean acquisition time between images. An example of this effect is shown for the SUP coordinate in Table 3. Indeed, Σ and μ were fitted to a linear

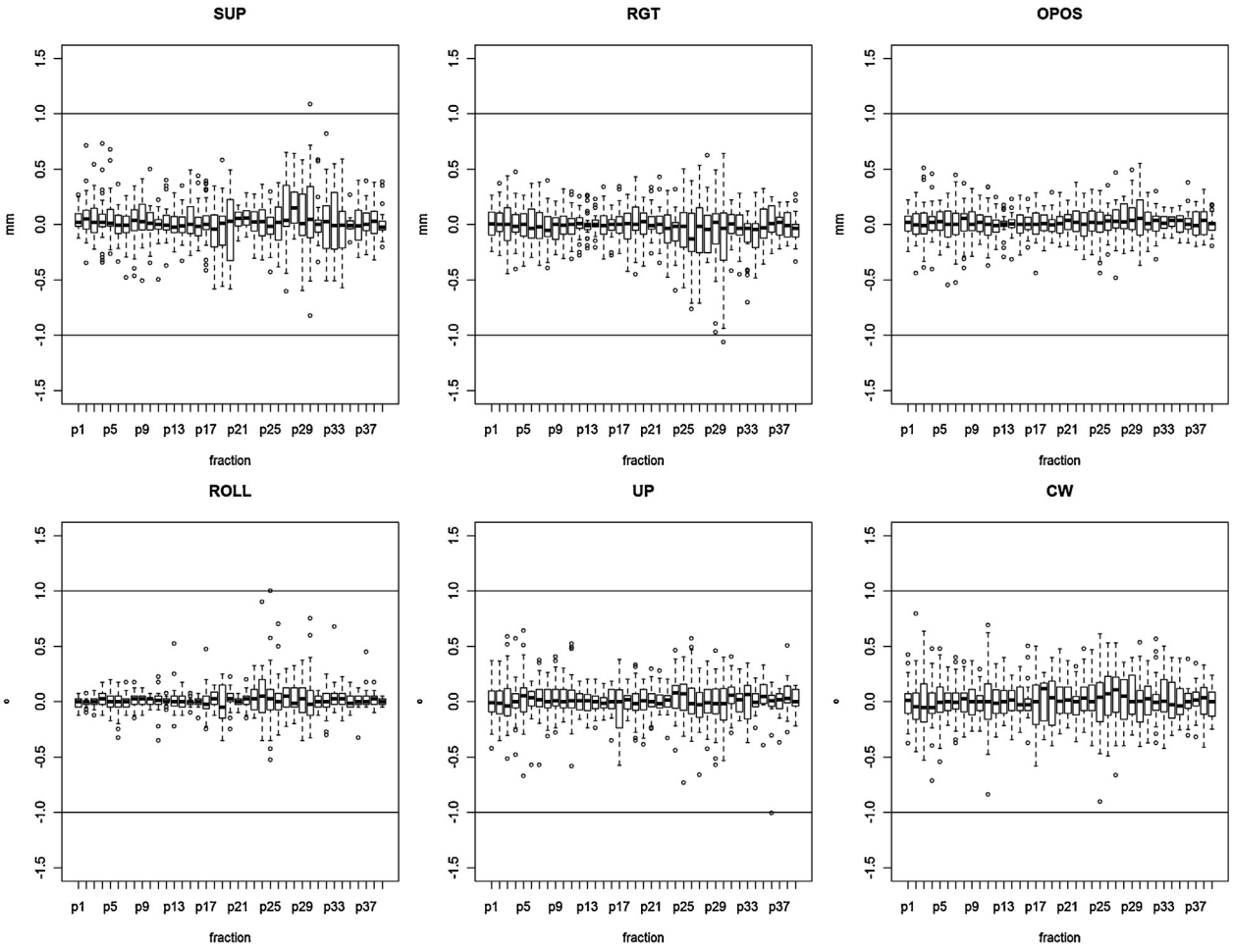

Fig. 1 – Boxplot diagram of the correction movement set for the 39 fractions analyzed.

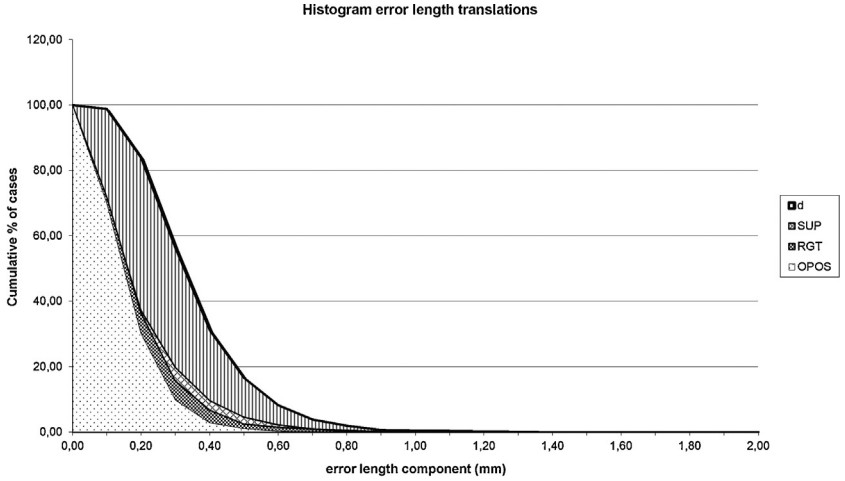

Fig. 2 – Histogram of the error movement per translation components and 3D misalignment error (*d*).

model with respect to $\langle \Delta t \rangle$, with $r > 0.97$ and $p < 0.01$ in all the 3D coordinates (translations and rotations). For the random component σ, a better fit was observed to the linear model ($r > 0.99$, $p < 0.005$), with estimated coefficient parameters in the range of 0.07–0.10 for translations and 0.03–0.05 for rotations.

5. Discussion

Traditional frame-based radiosurgery has a global accuracy of 1–2 mm. The X-ray image-guided CyberKnife VSI frameless radiosurgery system has an overall accuracy of less than

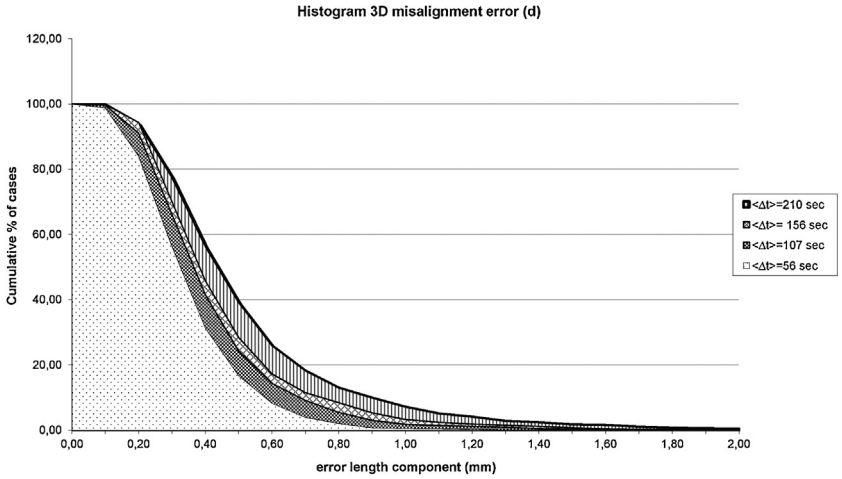

Fig. 3 – Histogram of the 3D misalignment error (*d*) as a function of the mean time between image acquisitions.

1 mm based on anthropomorphic head phantom end-to-end (E2E) measurements.[5] In our case, the E2E measurements made since the machine was commissioned show a technical accuracy of 0.48 mm (standard deviation, ±0.23; $n = 15$), thus meeting the system requirements for frameless radiosurgery.

Evaluation of clinical global accuracy requires a deeper knowledge of intrafraction patient movement, as it is unfeasible to assume no target movement with the immobilization mask. We believe that overall accuracy can only be guaranteed when technical quality assurance is supported by acquisition data from real patients.

The movement distribution obtained in Fig. 2 and the results in Table 2 are comparable to or lower than those in other studies of patient movement with the CyberKnife VSI system.[9,10] Overall mean error was lower than 0.03 mm in the 3 axes, thus revealing no general drawbacks in the process. Consequently, we can say that, with similar systematic and random errors, there are no preferred axes of movement in the patient population for translations or rotations. These findings are also consistent with those of Hoogeman et al.,[9] namely, that the histogram of the 3D intrafraction displacement magnitude *d* and the systematic and random components enable us to conclude that the criterion of 1 mm is met during the complete fraction for all the patients treated to date in our department. No displacement error higher than 1.7 mm was found between consecutive images, and 99% of the displacements were lower than 0.85 mm.

The results for rotational errors are similar to those for translational errors. It is important to highlight the difficulty in quantifying the global effect of these rotational errors on global dose accuracy. Rotations are obtained from a geometric transformation with the coordinate origin in the CyberKnife VSI alignment center; therefore, the effect of the dose is associated with the distance from the target to this point.

We compared our results with those of previous studies on intrafraction patient movement in the CyberKnife VSI system.[9,13] With regard to the 3D alignment error histogram (Fig. 2), we found that our results were very similar to the $\Delta t = 1$ min found by Hoogeman et al.,[6] but half as wide (mean vector length of 0.25 mm) as that reported by Murphy et al.[13] Hoogeman et al. present a series of possible reasons for these discrepancies. In our opinion, these can be explained by the use of a different mask and immobilization procedure.

With regard to the linear association between population movement components and mean acquisition time, our results differed from those obtained by Hoogeman et al.[9] The 2 possible explanations for these discrepancies are as follows: on the one hand, the results obtained by those authors are based on the use of discrete bin time intervals (Δt), whereas we performed the analysis using mean time intervals ($\langle \Delta t \rangle$); on the other hand, we only simulated data until $\langle \Delta t \rangle = 3.54$ min, as we were interested in clinical application and CyberKnife VSI does not permit Δt acquisition values of more than 150 s (2.5 min). We consider that our results are valid in this time range. Comparison of the results of Hoogeman et al.[9] (especially Fig. 5 from their article) with ours leads us to believe that their results would have been similar to ours if they had restricted their analysis to the time interval we applied. Differences begin to appear with Δt higher than approximately 4 min, which is outside our study range.

Table 3 – Mean, systematic and random errors for the SUP coordinate as a function of the mean acquisition time between images.

	μ^T (mm)	Σ^T (mm)	σ^T (mm)
$\langle \Delta t \rangle = 56$ s	0.022	0.042	0.202
$\langle \Delta t \rangle = 107$ s	0.045	0.086	0.250
$\langle \Delta t \rangle = 156$ s	0.064	0.130	0.299
$\langle \Delta t \rangle = 210$ s	0.087	0.173	0.342

6. Conclusions

On the basis of the 3D error histogram, the systematic and random error components, and the E2E results for the registration algorithm, we can conclude that if CyberKnife VSI is applied using our previously defined immobilization and acquisition procedure, it can prove to be as accurate as frame-based radiosurgery systems and even more accurate than other frameless

radiosurgery systems.[15] The degree of accuracy was similar to that of frame-based radiosurgery, and the disadvantages associated with the technique[16] can be eliminated.

Conflict of interest

None declared.

Financial disclosure

None declared.

Acknowledgment

The authors would like to thank Mr. Thomas O'Boyle for his help in preparing this manuscript.

REFERENCES

1. Schell MC, Bovqa FJ, Larson DA, et al. Stereotactic radiosurgery. *AAPM Task Group 43 Report*, vol. 54. Boston: American Association of Physicist in Medicine; 1995:6–8.
2. Wysocka A. Physical aspects of treatment planning in linac-based radiosurgery of intracranial lesions. Review paper. *Rep Pract Oncol Radiother* 1998;**3**(3):59–66.
3. Murphy MJ. An automatic six-degree-of-freedom image registration algorithm for image-guided frameless stereotaxic radiosurgery. *Med Phys* 1997;**24**:857–66.
4. Joseph B, Supe S, Ramachandra A. CyberKnife: a double edged sword? *Rep Pract Oncol Radiother* 2010;**15**:93–7.
5. Kilby W, Dooley JR, Kuduvalli G, et al. The CyberKnife Robotic Radiosurgery System in 2010. *Technol Cancer Res Treat* 2010;**9**:433–52.
6. Chang SD, Main W, Martin D, et al. An analysis of the accuracy of the CyberKnife: a robotic frameless stereotactic radiosurgical system. *Neurosurgery* 2003;**52**:139–47.
7. Fu D, Kuduvalli G. A fast, accurate, and automatic 2D–3D image registration for image-guided cranial radiosurgery. *Med Phys* 2008;**35**:2180–94.
8. Adler JR, Murphy MJ, Chang SD. Image-guided robotic radiosurgery. *Neurosurgery* 1999;**44**:1299–307.
9. Hoogeman MS, Nuyttens JJ, Levendag PC, et al. Time dependence of intrafraction patient motion assessed by repeat stereoscopic imaging. *Int J Radiat Oncol Biol Phys* 2007:1–10.
10. Murphy MJ. Intrafraction geometric uncertainties in frameless image-guided radiosurgery. *Int J Radiat Oncol Biol Phys* 2009:1–5.
11. Antypas C, Pantelis E. Performance evaluation of a CyberKnife G4 image-guided robotic stereotactic radiosurgery system. *Phys Med Biol* 2008;**53**:4697–718.
12. Dieterich S, Gibbs IC. The CyberKnife in clinical use: current roles, future expectations. *Front Radiat Ther Oncol* 2011;**43**:181–94.
13. Murphy MJ, Chang SD, Gibbs IC. Patterns of patient movement during frameless image-guided radiosurgery. *Int J Radiat Oncol Biol Phys* 2003;**55**:1400–8.
14. De Boer H, Van Sörnsen J, Senan S. Analysis and reduction of 3D systematic and random setup errors during the simulation and treatment of lung cancer patients with CT-based external beam radiotherapy dose planning. *Int J Radiat Oncol Biol Phys* 2001;**49**:857–68.
15. Ramakrishna N, Rosca F, Friesen S. A clinical comparison of patient setup intra-fraction motion using frame-based radiosurgery versus a frameless image-guided radiosurgery system for intracranial lesions. *Radiother Oncol* 2010;**95**:109–15.
16. Otto K, Fallone BG. Frame slippage verification in stereotactic radiosurgery. *Int J Radiat Oncol Biol Phys* 1998;**41**:199–205.